Supplementary Information for

Stomach Curvature is Generated by Left-Right Asymmetric Gut Morphogenesis

Adam Davis, Nirav M. Amin, Caroline Johnson, Kristen Bagley, Troy Ghashghaei, Nanette Nascone-Yoder

Supplementary Materials and Methods

Mouse Genotyping

Phenol-choloroform-isoamyl alcohol extraction was used to obtain genomic DNA from embryonic yolk sacs. PCR primers used were:

GCE Forward – 5' CTC CCA CAT CAGGCA CAT GAG TAA 3'

GCE Reverse – 5' GCA AACAAC AGA TGG CTG GCA ACT 3'.

Xenopus Loss-of-function

The following morpholino sequences were used.

#1 (targets the *pitx2c* 5'UTR):	5'-ggtacagtacagtaggctcacagac-3'
#2 (targets the *pitx2c* ATG start site):	5'-gtaaagggtctttcatagagttcat-3'
Control (Genetools):	5'-cctcttacctcagttacaatttata-3'.

For CRISPR-Cas9 experiments, Tyrosinase gRNA was used as a positive control (Guo et al., 2014). *pitx2c* gRNA target sites were:

#1 GGAGTGTAAGTCAAGGCTAGAGG

#2 GGTGATGATGGTGGTGGTGATGG.

PCR primers used to amplify the *pitx2c* genomic locus targeted by gRNAs #1 and 2 were:

fwd 5'-GGCACCTGCCTTTAATGCTC- 3'

rev 5'-CACACCTGTGAGTAATCAGC- 3'.

Amplicons were denatured and allowed to slowly cool to allow formation of heteroduplex of wild-type and mutant products. Heteroduplexes were identified by digesting the product with T7 endonuclease I (NEB) as previously described (Guo et al., 2014). Uncut PCR products were subcloned into pCR2.1 vector (ThermoFisher Scientific) and individual clones were sequenced with M13R (5'-CAGGAAACAGCTATGAC-3') to determine mutation frequency. Sequencing was performed at the Eton Bioscience (Research Triangle Park, NC, USA).

Antibodies

Primary antibodies used for immunohistochemistry include anti-β-catenin (Santa Cruz, sc-7199, 1:100), anti-α-tubulin (Sigma, T9026, 1:1000), anti-aPKC (Santa Cruz, sc-216, 1:200), anti-integrin (Developmental Studies Hybridoma Bank, DSHB, , created by the NICHD of the NIH and maintained at The University of Iowa; 8C8, 1:1000), anti-γ-tubulin (Abcam, ab27074, 1:1000), anti-phospho-histone H3 (pHH3; Millipore, 06-570, 1;500), anti-E-cadherin (DSHB, 5D3-c, 1:200) and anti-Par3 (Millipore, 07-330, 1:200). Secondary antibodies used were Alexa 488-conjugated goat anti-mouse IgG (Invitrogen, A11029; 1:2000) and/or Alexa 546-conjugated goat anti-rabbit IgG (Invitrogen, A11035; 1:2000). Nuclear staining was accomplished with TO-PRO-3 Iodide (T3605; 1:1000).

Antibodies used in Western blotting were rabbit anti-GFP (ThermoFisher, A6455, 1:1000), rabbit anti-GAPDH (Millipore, AB2302, 1:1000), and HRP-conjugated donkey anti-rabbit IgG (ThermoFisher, A16035, 1;10,000).

Methodology and Statistics

To ensure adequate power, at least 30 *Xenopus* embryos were used for each group/condition in each experiment. Mouse sample size was dependent on litter size from two independent breedings.

For *Xenopus* loss- and gain-of-function studies, embryos from a single clutch were randomly allocated to control or experimental groups; each experiment was performed at least 3 times, using independent breedings, with similar results.

For both mouse and *Xenopus* studies, results were validated by an independent researcher blinded to group allocation.

For mouse morphometric measurements, 2-3 sections were analyzed from at least 2 embryos. For *Xenopus* morphometric measurements, 2-3 sections were analyzed from at least 3 embryos.

For most analyses, a one-way Anova with post-hoc Tukey honest significant difference (HSD) was calculated, validated with additional Scheffé, Bonferroni and Holm multiple comparisons.

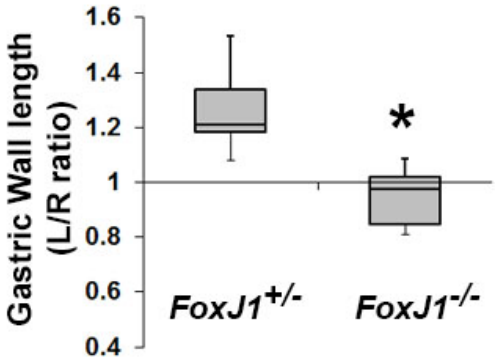

Figure S1. The normal left/right ratio of the lengths of the stomach walls is eliminated in E11.5 *FoxJ1*$^{-/-}$ mouse stomachs (* denotes p<0.01).

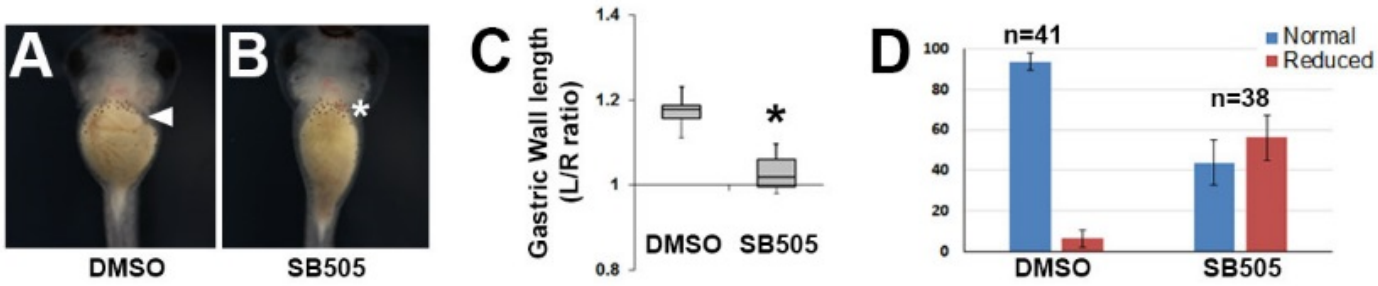

Figure S2. SB505124 exposure inhibits stomach curvature. Stage 19/20 frog embryos were exposed to DMSO (**A**) or 5μM SB505124 (**B**) through stage 42. **C**) The normal left/right (L/R) ratio of the lengths of the stomach walls is eliminated in SB505124-dosed embryos (* denotes $p<0.01$). The graph (**D**) indicates the percentage of embryos in which the greater curvature of the stomach is normal (e.g., arrowhead in **A**) or reduced/absent (* in **B**).

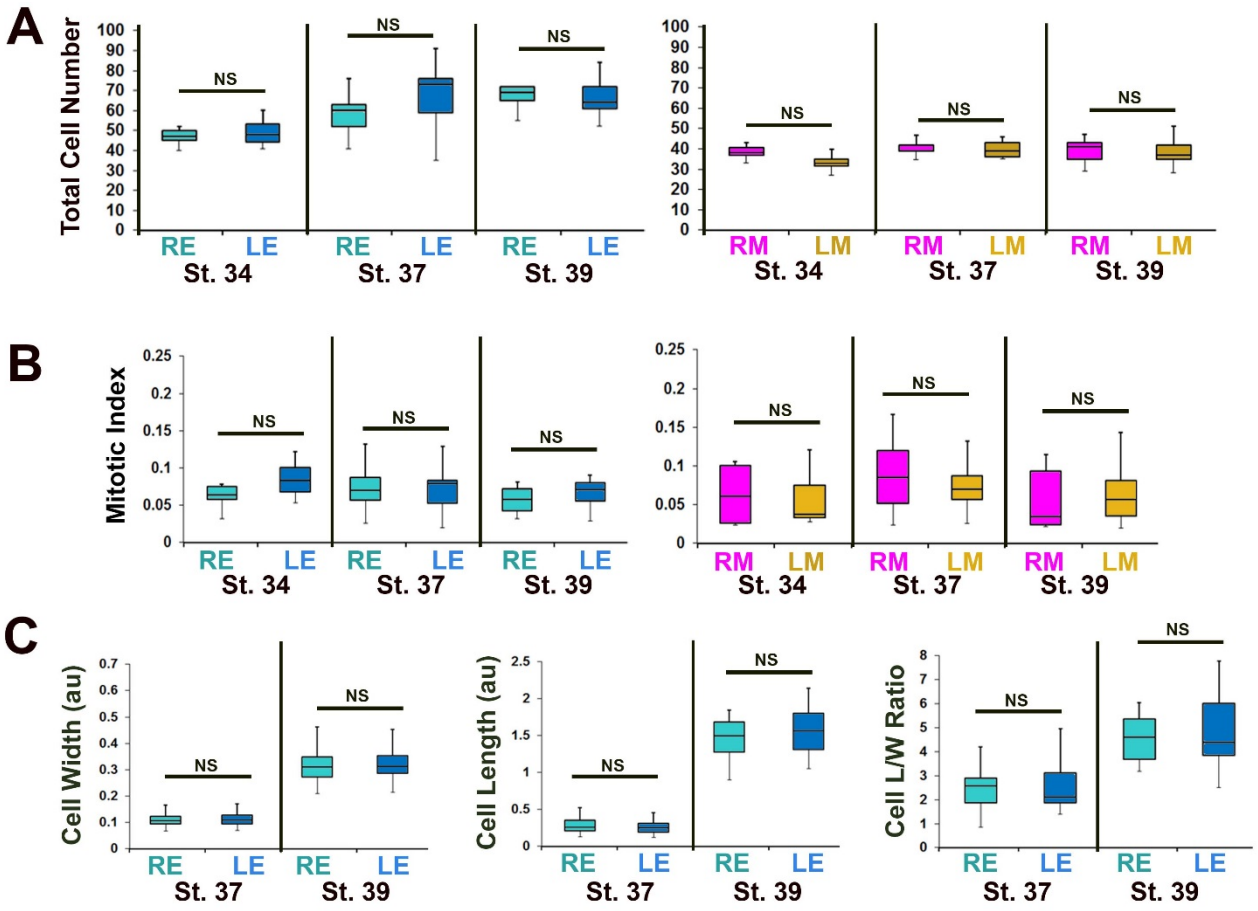

Figure S3. Morphometric comparison of cell properties in the left and right stomach walls. Sections of the developing stomach were immunohistochemically stained to reveal cell outlines or mitotic nuclei, and the indicated features were counted and/or measured at St. 34, 37 and 39, using at least 3 sections from each of 3 different embryos. At no stage are the total number of cells (**A**) or mitotic indices (**B**; number of pHH3+ cells/number of total cells) statistically different between the left and right sides. Likewise, there is no statistical difference in endoderm cell width, length or length/width (L/W) ratio between sides during curvature formation (**C**). RE, right endoderm; LE, left endoderm; RM, right mesoderm; LM, left mesoderm

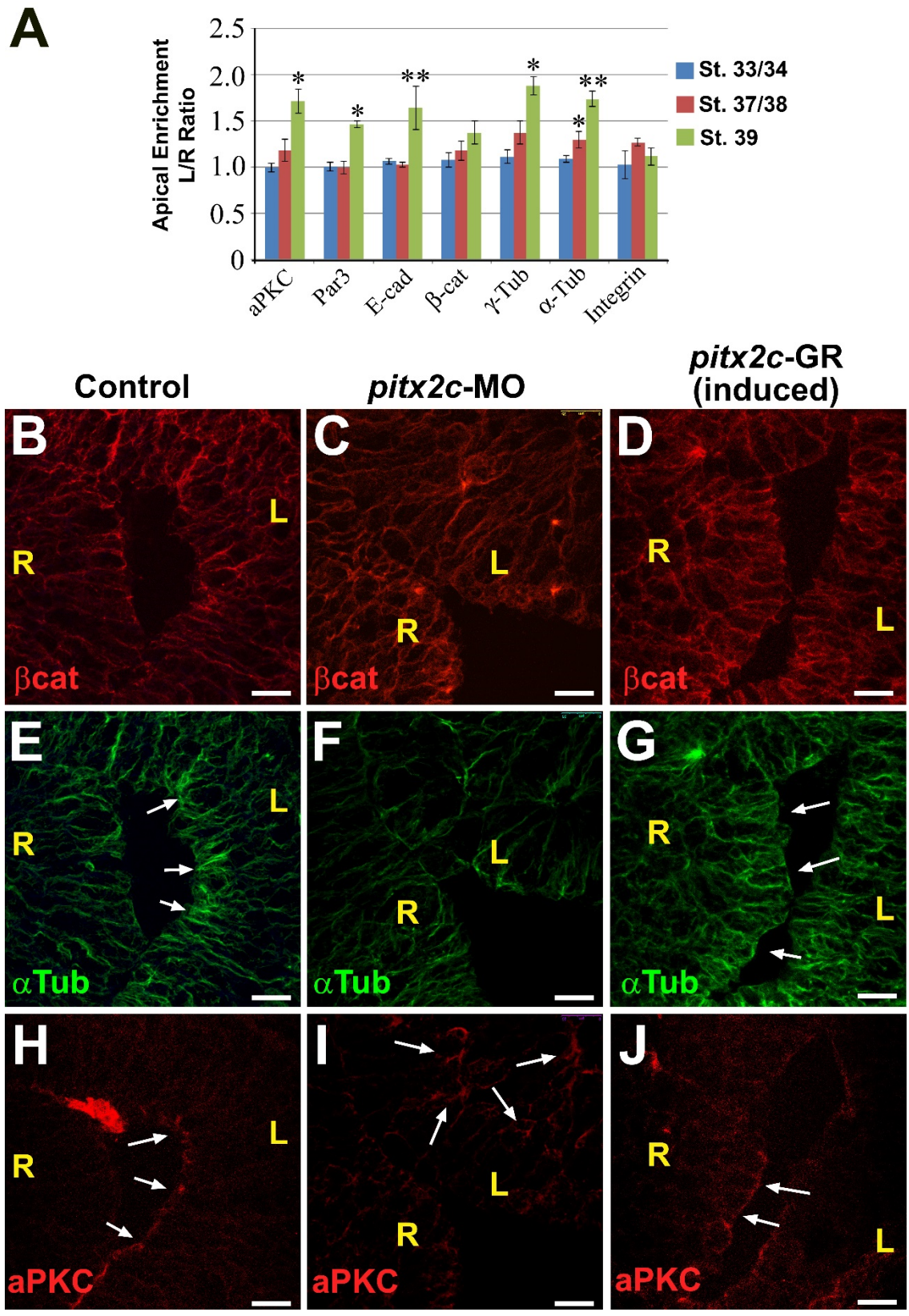

Figure S4. Markers of apicobasal polarity become left-right asymmetric in the developing stomach. The intensity of several markers of apical polarity, including aPKC, Par3, E-cadherin (E-cad), α-tubulin (α-tub) and γ-tubulin (γ-tub) were measured at the left and right surfaces of the frog stomach lumen at the indicated stages

using image J **(A)**. The level of apical enrichment is represented as a ratio of left and right intensities measured in at least 3 sections of 3-5 different embryos. The left/right (L/R) ratios of all apical markers become significantly different by stage 39, while the L/R ratios of β-catenin (β-cat) and integrin are not significantly >1. **B-J**) High magnification images of sections through the Stage 39 stomach stained for β-catenin (βcat; red; **B-D**), α−tubulin (αtub; green; **E-G**), or atypical PKC (aPKC; red; **H-J**). Compared to control embryos (**B, E, H**), in which αtub and aPKC are concentrated at the apical surface of the left stomach wall (arrowheads in **E, H,** respectively), MO depletion of Pitx2c (**C, F, I**) disrupts epithelial architecture (arrows in **I**). Meanwhile, dexamethasone-induction of Pitx2c activity (**D, G, J**) in the right wall ectopically polarizes the stomach endoderm, as indicated by ectopic regions of polarized epithelial architecture, correlating with enriched αtub and ectopic aPKC at the apical surface (arrows in **G, J**). Scalebars = 25uM. Left (L), Right (R).

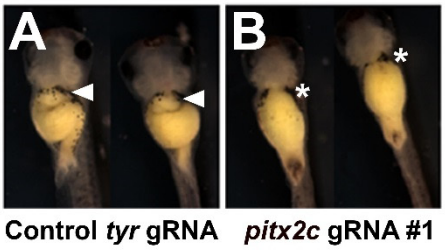

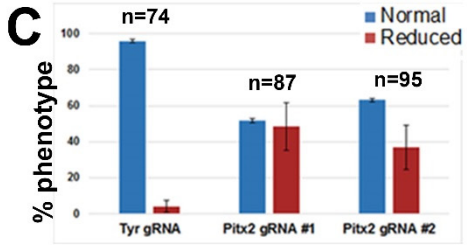

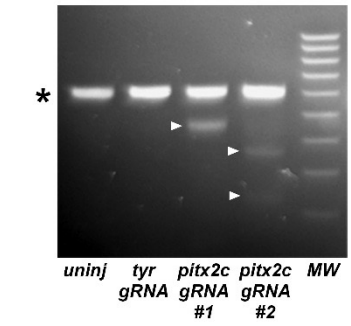

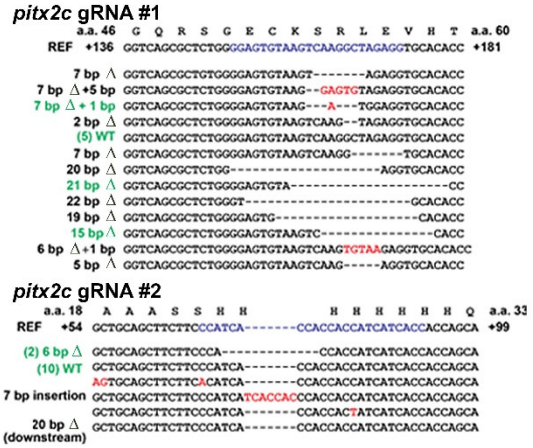

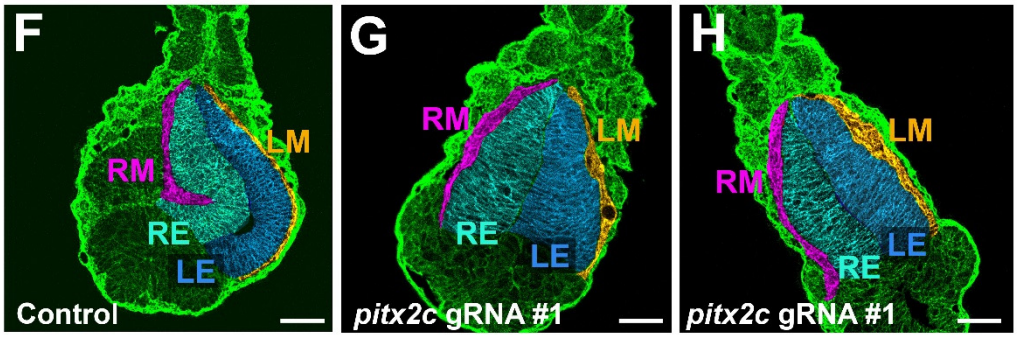

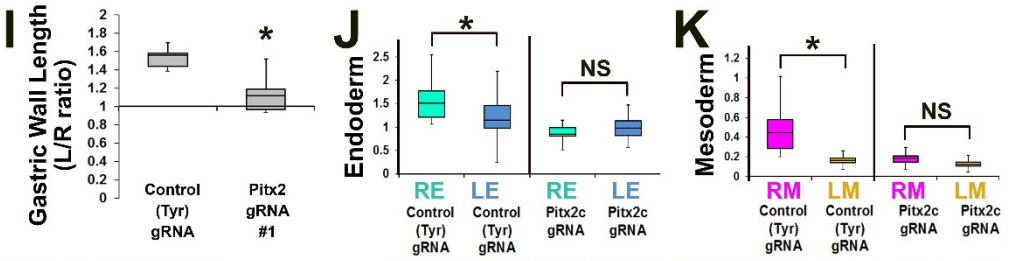

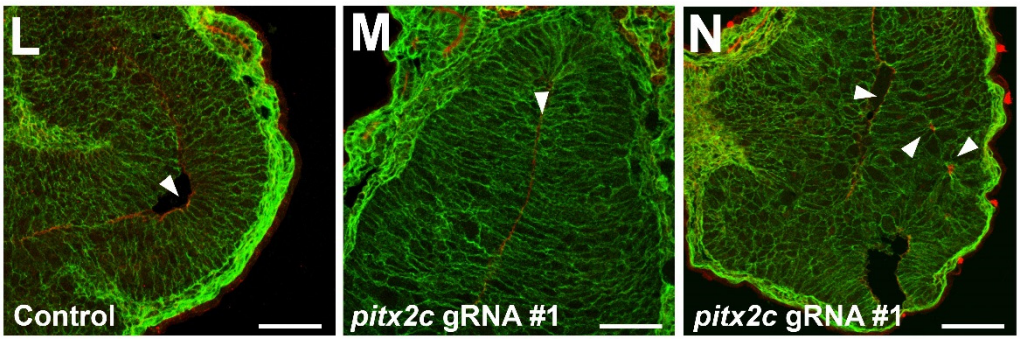

Figure S5. CRISPR-Cas9 mediated editing of *pitx2c* gene perturbs stomach asymmetry. *Xenopus* embryos were injected with 2 ng synthetic Cas9 mRNA plus 300 pg control *tyrosinase (tyr)* gRNA (**A**) or *pitx2c* gRNA (**B**), and allowed to develop until stage 42. The graph (**C**) indicates the percentage of embryos in which the greater curvature of the stomach is normal (arrowhead in **A**) or reduced/absent (* in **B**) after injection with the *tyr* gRNA or two different *pitx2*c gRNAs (#1 and #2). **D**) Genomic DNA from 10 embryos injected with each gRNA was pooled and PCR amplified using exon 1-specific primers, and then tested for CRISPR/Cas9-induced mutations by T7 endonuclease I assay. The asterisk (*) indicates the 500 bp amplicon not cut in un-injected or *tyr* gRNA-injected control embryos. Arrowheads indicate bands resulting from mismatches (inferred mutations) in amplicons cleaved by T7 endonuclease I. **E**) Sequencing of a subset of individual clones validates the presence of deleterious mutations in *pitx2c* gRNA injected embryos. For *pitx2c* gRNA #1, 9/17 mutations were likely nulls and 3/17 were predicted to result in compromised function; for *pitx2c* gRNA #2: 2/18 mutations were likely nulls and 4/17 were likely to result in compromised function. **F-N**) Sections through stomachs of Cas9 control and *pitx2c* gRNA (#1) injected embryos (Stage 39) were stained for integrin (green) and false color-coded as in Fig. 1 to highlight the relevant tissue layers (RE, right endoderm; LE, left endoderm; RM, right mesoderm; LM, left mesoderm). Controls show normal asymmetric expansion of the left stomach wall (**F**), but this is eliminated in embryos injected with *pitx2c* gRNA (**G-H**). Normal asymmetries in the lengths of the left and right stomach walls (**I**), and the widths of the endoderm (Endo) and mesoderm (Meso) layers (**J-K**), are also significantly perturbed by CRISPR-Cas editing of *pitx2c*; * denotes $p<0.01$. Compared to controls (**L**), left endoderm tissue architecture is severely disrupted, and apicobasal polarity is reduced (**M**), and/or disorganized (**N**) in embryos with CRISPR-mediated mutations in *pitx2c*; arrowheads indicate the expression of the apical marker aPKC (red). Scalebars= 100 μM.

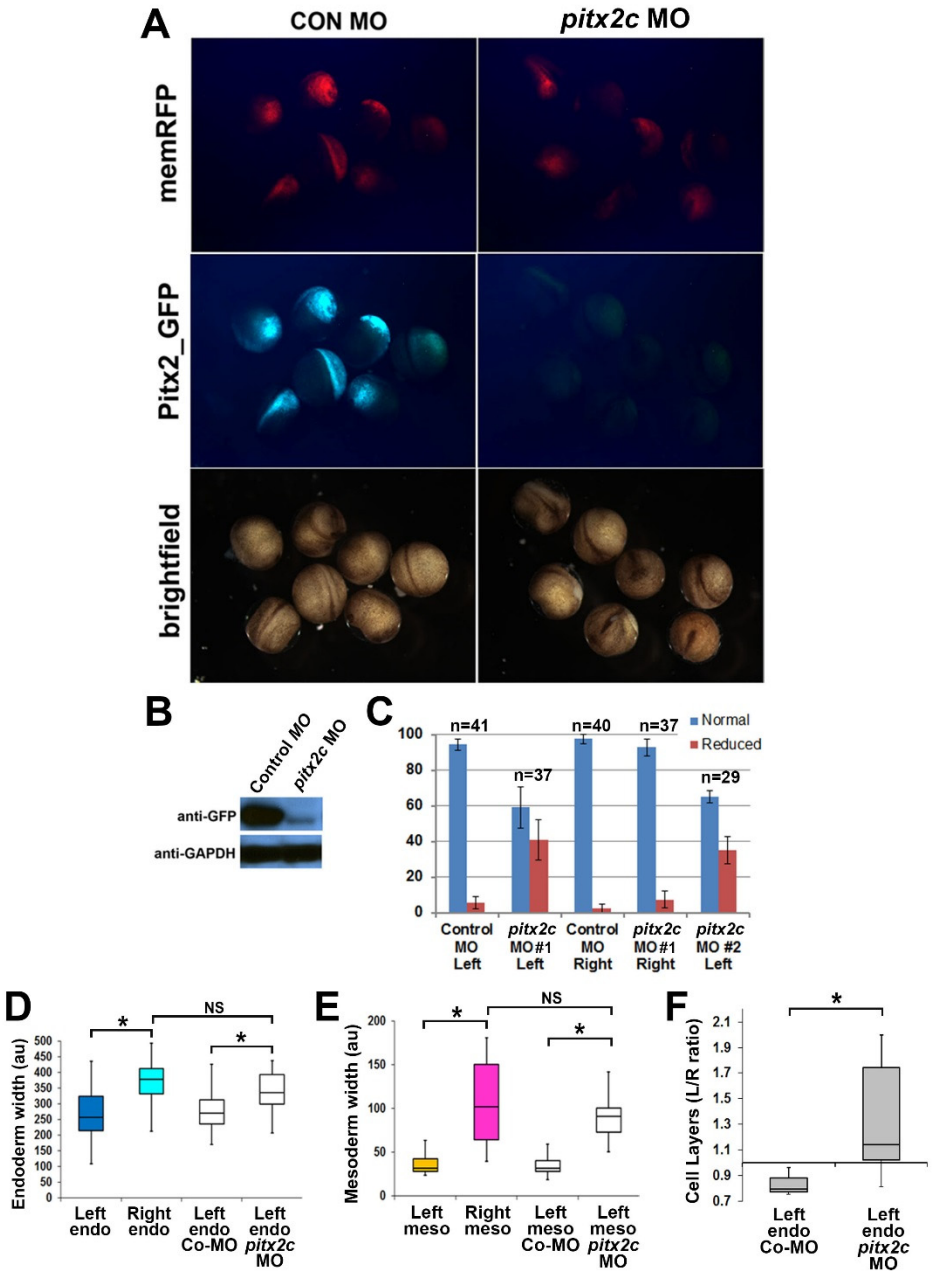

Figure S6. Specificity and efficacy of the *pitx2c* MO. A) *Xenopus* embryos (8-cell stage) were injected with 8 ng Control or *pitx2c* MO plus 200pg RFP mRNA and GFP mRNA (fused with *pitx2c* 5' UTR MO target site), and cultured until stage 20. Effective translation, indicated by GFP fluorescence, is visible in embryos injected with Control MO, but not with *Pitx2c* MO; RFP (which does not contain the *pitx2c* 5' UTR sequence) levels remain unaffected. **B**) Western blot confirms drastic reduction of GFP protein levels in embryonic extracts from *pitx2c*-MO- but not Control-MO-injected embryos. GAPDH, loading control. **C**) The graph indicates the frequency (percentage) of embryos in which the greater curvature of the stomach is normal or reduced/absent when Control MO or *pitx2c*-MO (#1) is targeted to either the left or right side. A second, independent MO (*pitx2c* MO #2) confirmed the result. While injection of Control MO has no effect on the relative thickness of the left endoderm (**D**) or mesoderm (**E**), *pitx2c*-MO-injected tissues are similar in thickness to the normal (non-*pitx2c*-expressing) right tissues (i.e., not significantly different, NS). **F**) The L/R ratio of endoderm cell layers is significantly increased in *pitx2c*-MO-injected stomachs, compared to Control-MO. * denotes $p<0.01$

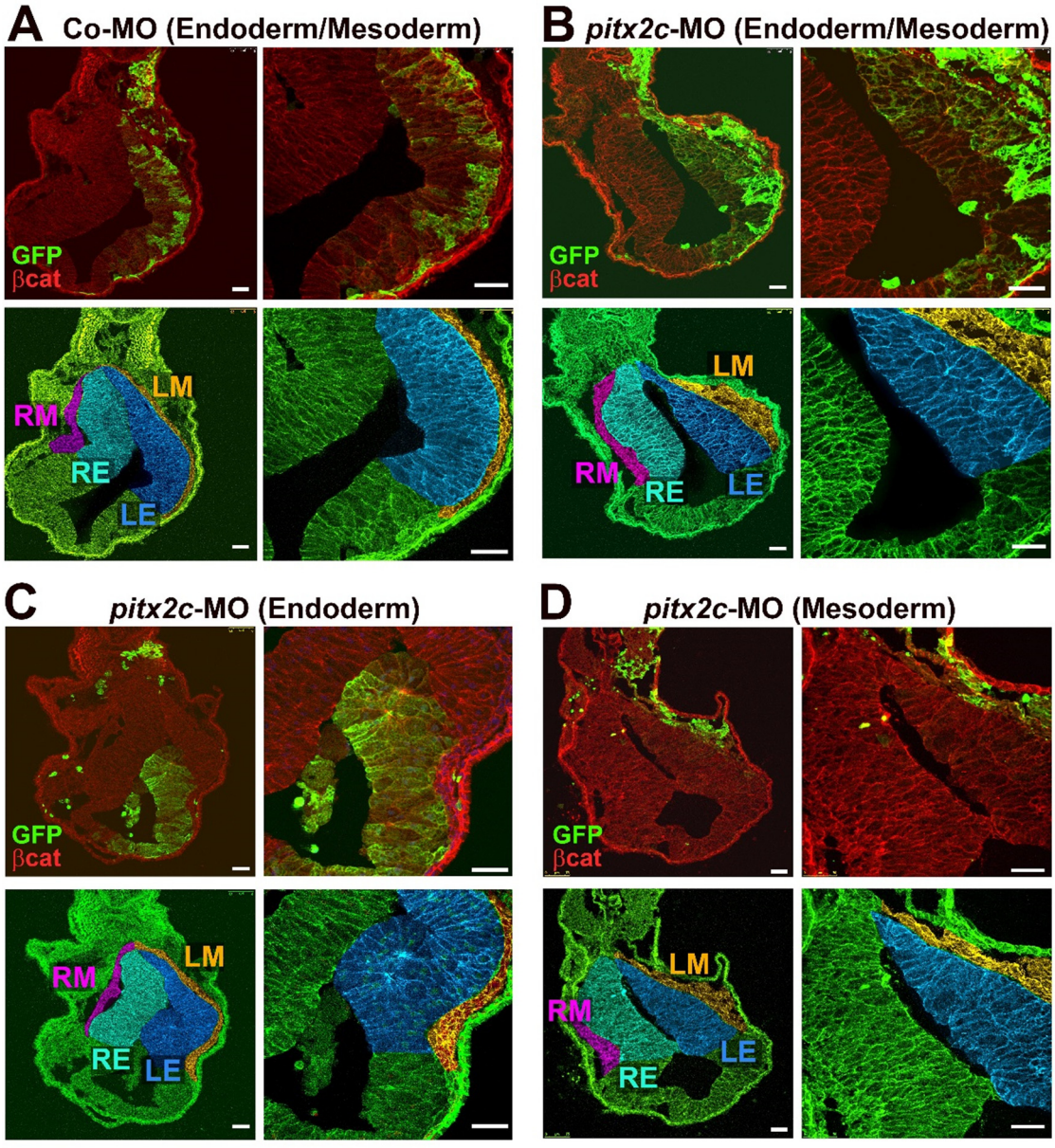

Figure S7. Reciprocal endoderm-mesoderm interactions affect morphogenesis of the left stomach wall. Frog embryos were injected with GFP mRNA and either control morpholino (Co-MO; **A**) or *pitx2c*-MO (**B-D**), targeted to the left side of the stomach. Top panels: sections through the stomach were stained for β-catenin (βcat; red) and GFP (green). Bottom panels: the same sections were false color-coded as in Fig. 1(b) to highlight the relevant tissue layers (RE, right endoderm; LE, left endoderm; RM, right mesoderm; LM, left mesoderm). In the embryo shown in **A**, Control-MO is distributed throughout the LE and LM of the left stomach wall, which exhibits normal left side tissue architecture. In the embryo shown in **B**, *pitx2c*-MO is distributed throughout the LE and LM, and both tissue layers are abnormally thickened and/or disorganized. In **C**, *pitx2c*-MO is present predominately in the LE, with minimal contribution to the LM; yet, both the LE and LM are abnormal. Likewise, in **D**, *pitx2c*-MO is present only in the LM, with minimal contribution to LE, but both LE and LM are abnormal.